

cross-linking the material makes it possible to assemble composite structures that differ by as little as a single monolayer (one monomer thick). In addition to uses as models of superabsorbing polymer networks (8) and in bioadsorption studies (9), these materials should be ideal for the flexible hydrophilic spacing layers needed between supported bilayers and solid substrates for biologically relevant studies of the physical properties of membranes (22).

## REFERENCES AND NOTES

1. M. C. Petty, *Langmuir-Blodgett Films: An Introduction* (Cambridge Univ. Press, Cambridge, 1996); G. Roberts, Ed., *Langmuir-Blodgett Films* (Plenum, New York, 1990).
2. A. Ulman, *An Introduction to Ultrathin Organic Films: From Langmuir-Blodgett to Self-Assembly* (Academic Press, Boston, 1991); J. D. Swalen, *J. Mol. Electron.* **2**, 155 (1986).
3. W. M. K. P. Wijekoon *et al.*, *J. Am. Chem. Soc.* **118**, 4480 (1996); T. L. Penner, H. R. Motschmann, N. J. Armstrong, M. C. Ezenyilimba, D. Williams, *Nature* **367**, 49 (1994); K. Clays, N. J. Armstrong, T. L. Penner, *J. Opt. Soc. Am. B* **10**, 886 (1993); K. Clays, N. J. Armstrong, M. C. Ezenyilimba, T. L. Penner, *Chem. Mater.* **5**, 1032 (1993).
4. G. Wegner, *Mol. Cryst. Liq. Cryst.* **235**, 1 (1993).
5. R. Rulkens, G. Wegner, V. Enkelmann, M. Schulze, *Ber. Bunsenges. Phys. Chem.* **100**, 707 (1996).
6. M. Bardosova, R. H. Tredgold, Z. Ali-Adib, *Langmuir* **11**, 1273 (1995); A. Takahara *et al.*, *Macromolecules* **22**, 617 (1989).
7. M. Tamura and A. Sekiya, *Chem. Lett.* **1991**, 399 (1991).
8. K. S. Kazanskii and S. A. Dubrovskii, *Adv. Polym. Sci.* **104**, 97 (1992); R. Po, *Rev. Macromol. Chem. Phys.* **34**, 607 (1994).
9. A. Hartmann and S. Seeger, *Thin Solid Films* **245**, 206 (1994); H. Fukushima, H. Morgan, D. M. Taylor, *ibid.* **244**, 789 (1994); S. Seeger *et al.*, in *Synthetic Microstructures in Biological Research*, J. M. Schnur and M. Peckerar, Eds. (Plenum, New York, 1992), p. 586.
10. V. Buchholz *et al.*, *Langmuir* **13**, 3206 (1997); V. Buchholz, G. Wegner, S. Stemme, L. Ödberg, *Adv. Mater.* **8**, 399 (1996); M. Schaub, G. Wenz, G. Wegner, A. Stein, D. Klemm, *ibid.* **5**, 919 (1993).
11. J. E. Sutherland and M. L. Miller, *J. Polym. Sci. B* **7**, 871 (1969).
12. M. Sacchetti, H. Yu, G. Zografis, *Langmuir* **9**, 2168 (1993); S. Kim and H. Yu, *Progr. Colloid Polym. Sci.* **89**, 202 (1992); M. Kawaguchi, B. S. Bauer, H. Yu, *Macromolecules* **22**, 1735 (1989).
13. The three-arm PtBMA stars (bearing anthryl end groups), linear PtBMA ( $\alpha,\omega$ -*p*-vinylbenzyl-functionalized), and PtBA ( $\alpha,\omega$ -allyl-functionalized) (Fig. 1C) were prepared by anionic polymerization. The cellulose derivatives (IPCC and IPC) (Fig. 1D) were prepared and characterized according to the method of M. Schaub [thesis, University of Mainz, Mainz, Germany (1993)]. Gel permeation chromatography with poly(styrene)/divinylbenzene columns (SDV 500, PSS Inc.) with mesh sizes of  $10^3$ ,  $10^5$ , and  $10^6$  Å were used to deduce poly(methyl methacrylate) [poly(styrene) for the celluloses] standard number-average molecular weights ( $M_n$  in kilograms per mole) and polydispersities ( $M_w/M_n$ ) of PtBMA star (33.7, 1.04), linear PtBMA (25.8, 1.18), PtBA (28.8, 1.50), IPCC (89.2, 1.96), and IPC (114, 1.97). The functionality of the PtBMA (95%) and PtBA (85%) end groups was determined by a 300-MHz  $^1\text{H}$  nuclear magnetic resonance spectroscopy (Bruker). The cellulose derivatives had degrees of substitution of IPCC (2.1 isopentyl, 0.3 cinnamate, and 0.6 hydroxyl) and IPC (2.8 isopentyl, 0.2 hydroxyl) based on elemental analysis.
14. Transfer ratios of  $1.00 \pm 0.05$  onto Si substrates hydrophobized with ammonium fluoride (x-ray experiments) or 1,1,1,3,3,3-hexamethyldisilazane (infrared studies) were obtained for all of the samples under the following conditions (temperature in degrees centigrade, surface concentration in angstroms squared per monomer, surface pressure in millinewtons per meter): PtBMA star (20, 22.9, 12), linear PtBMA (8 and 20, 22.7, 15), PtBA (8, 26.3, 15), IPCC (8, 63.0, 15 and 18), and IPC (8, 67.8, 18).
15. The periodic fluctuations seen in Fig. 3 represent Kiessig fringes, which arise from the interference between x-rays reflected from the Si-polymer and polymer-air interfaces. Knowing the position of the maxima, one can obtain the thickness of the film [P. Tippmann-Krayer, H. Möhwald, Yu. M. L'vov, *Langmuir* **7**, 2298 (1991)]. A more detailed analysis obtained by directly fitting the experimental profiles with theoretical curves also yields the roughness of both the film and the substrate. For this study, we applied the latter technique using the methods and experimental set-up described in M. Schaub *et al.*, *Macromolecules* **28**, 1221 (1995).
16. D. W. van Krevelen and P. J. Hoftyzer, *Properties of Polymers: Their Estimation and Correlation with Chemical Structure* (Elsevier, Amsterdam, 1976).
17. IR spectroscopy was carried out on a Nicolet Magna 850 Fourier-transform with LB films (80 to 100 layers) deposited on Si hydrophobized with 1,1,1,3,3,3-hexamethyldisilazane.
18. S. Iida, M. Schaub, M. Schulze, G. Wegner, *Adv. Mater.* **5**, 564 (1993); P. L. Egerton, E. Pitts, A. Reiser, *Macromolecules* **14**, 95 (1981).
19. An easy and reliable test of whether a network forms is to take the cross-linked LB film and immerse it in a good solvent [M. Seufert, M. Schaub, G. Wenz, G. Wegner, *Angew. Chem. Int. Ed. Engl.* **34**, 340 (1995)]. When the film is not a network, the film is soluble and leaves the substrate.
20. G. Decher, *Science* **277**, 1232 (1997).
21. M. L. Bruening *et al.*, *Langmuir* **13**, 770 (1997); Y. Zhou, M. L. Bruening, Y. Liu, R. M. Crooks, D. E. Bergbreiter, *ibid.* **12**, 5519 (1996); Y. Zhou, M. L. Bruening, D. E. Bergbreiter, R. M. Crooks, M. Wells, *J. Am. Chem. Soc.* **118**, 3773 (1996).
22. H. Sigl *et al.*, *Eur. Biophys. J.* **25**, 249 (1997); E. Sackmann, *Science* **271**, 43 (1996).
23. Financial support was provided by the Stockhausen GmbH & Co. KG.

16 December 1997; accepted 12 March 1998

## The Biochemical Basis of an All-or-None Cell Fate Switch in *Xenopus* Oocytes

James E. Ferrell Jr.\* and Eric M. Machleder

*Xenopus* oocytes convert a continuously variable stimulus, the concentration of the maturation-inducing hormone progesterone, into an all-or-none biological response—oocyte maturation. Here evidence is presented that the all-or-none character of the response is generated by the mitogen-activated protein kinase (MAPK) cascade. Analysis of individual oocytes showed that the response of MAPK to progesterone or Mos was equivalent to that of a cooperative enzyme with a Hill coefficient of at least 35, more than 10 times the Hill coefficient for the binding of oxygen to hemoglobin. The response can be accounted for by the intrinsic ultrasensitivity of the oocyte's MAPK cascade and a positive feedback loop in which the cascade is embedded. These findings provide a biochemical rationale for the all-or-none character of this cell fate switch.

Fully grown *Xenopus laevis* oocytes are arrested in a state that resembles the  $G_2$  phase of the cell division cycle with inactive cyclin-dependent kinase Cdc2 and an intact germinal vesicle. Exposure to the hormone progesterone induces oocytes to undergo maturation, during which they activate Cdc2, undergo germinal vesicle breakdown, complete the first meiotic division, and finally arrest in metaphase of meiosis 2 (1). Oocyte maturation is an example of a true cell fate switch; oocytes can reside in either the  $G_2$  arrest or the metaphase arrest state for extended periods of time, but can be in intermediate states only transiently.

Progesterone-induced maturation is thought to be triggered by activation of a cascade of protein kinases—Mos, Mek-1, and p42 or Erk2 MAP kinase (MAPK). Progesterone causes the accumulation of

Mos, which phosphorylates and activates Mek-1. Active Mek-1 in turn phosphorylates and activates p42 MAPK, which brings about activation of the Cdc2–cyclin B complex. Interfering with the accumulation of Mos (2) or the activation of Mek-1 (3) or p42 MAPK (4) inhibits progesterone-induced activation of Cdc2 and maturation, and microinjection of nondegradable Mos (5), constitutively active Mek-1 (4, 6), or thiophosphorylated p42 MAPK (7) brings about Cdc2 activation and maturation in the absence of progesterone. At some point in this chain of events, a continuously variable stimulus—the progesterone concentration—is converted into an all-or-none biological response.

Studies of the steady-state responses of the MAPK cascade in *Xenopus* oocyte extracts indicate that the cascade might contribute to the all-or-none character of oocyte maturation. In extracts, the response of MAPK to recombinant malE-Mos (a maltose-binding protein Mos fusion protein) is highly ultrasensitive (8), meaning it resem-

Department of Molecular Pharmacology, Stanford University School of Medicine, Stanford, CA 94305-5332, USA.

\*To whom correspondence should be addressed. E-mail: ferrell@cmgm.stanford.edu

bles that of a positively cooperative enzyme (9). The apparent Hill coefficient ( $n_H$ , a measure of the ultrasensitivity) for the MAPK response is about 5 (8). This is a large Hill coefficient; the benchmark is the Hill coefficient for oxygen binding by hemoglobin, which is about 2.8 (10). The ultrasensitivity arises in part from the fact that MAPK requires the phosphorylation of two sites for activation (11, 12), and it increases nearly multiplicatively as the cascade is descended (13). An ultrasensitive system behaves more like a switch than a Michaelian ( $n_H = 1$ ) system does—the response to small stimuli is minimal, but once the system begins to respond, it switches from off to on over a narrower range of stimulus concentrations than does a Michaelian system (Fig. 1G). Thus, the MAPK cascade might contribute to the all-or-none character of oocyte maturation, provided ultrasensitivity is exhibited by MAPK in intact oocytes as well as extracts.

We, therefore, assessed the phosphorylation of p42 MAPK in groups of oocytes treated with different concentrations of progesterone (14). The overall response appeared to be no more switchlike than that of a typical Michaelian system ( $n_H \approx 1$ , Fig. 1A). However, a problem arises in interpreting the response of a potentially heterogeneous population. A graded overall response could mean that each of the individual oocytes had a graded response (Fig. 1B), but

even if individual oocytes had perfectly switchlike responses, samples of oocytes would yield a graded response if the oocytes varied with respect to the concentration of progesterone required to switch them on (Fig. 1C).

These two possibilities can be distinguished by examining individual oocytes treated with intermediate concentrations of progesterone. If the individual responses are graded, each oocyte should have an intermediate amount of MAPK phosphorylation (Fig. 1B); if they are switchlike, the oocytes should have either very high or very low levels of MAPK phosphorylation (Fig. 1C). This argument can be translated into a mathematical formula (15) for inferring the steepness (value of  $n_H$ ) of the oocytes' individual responses from the observed distribution of responses in a sample of oocytes (Fig. 1D).

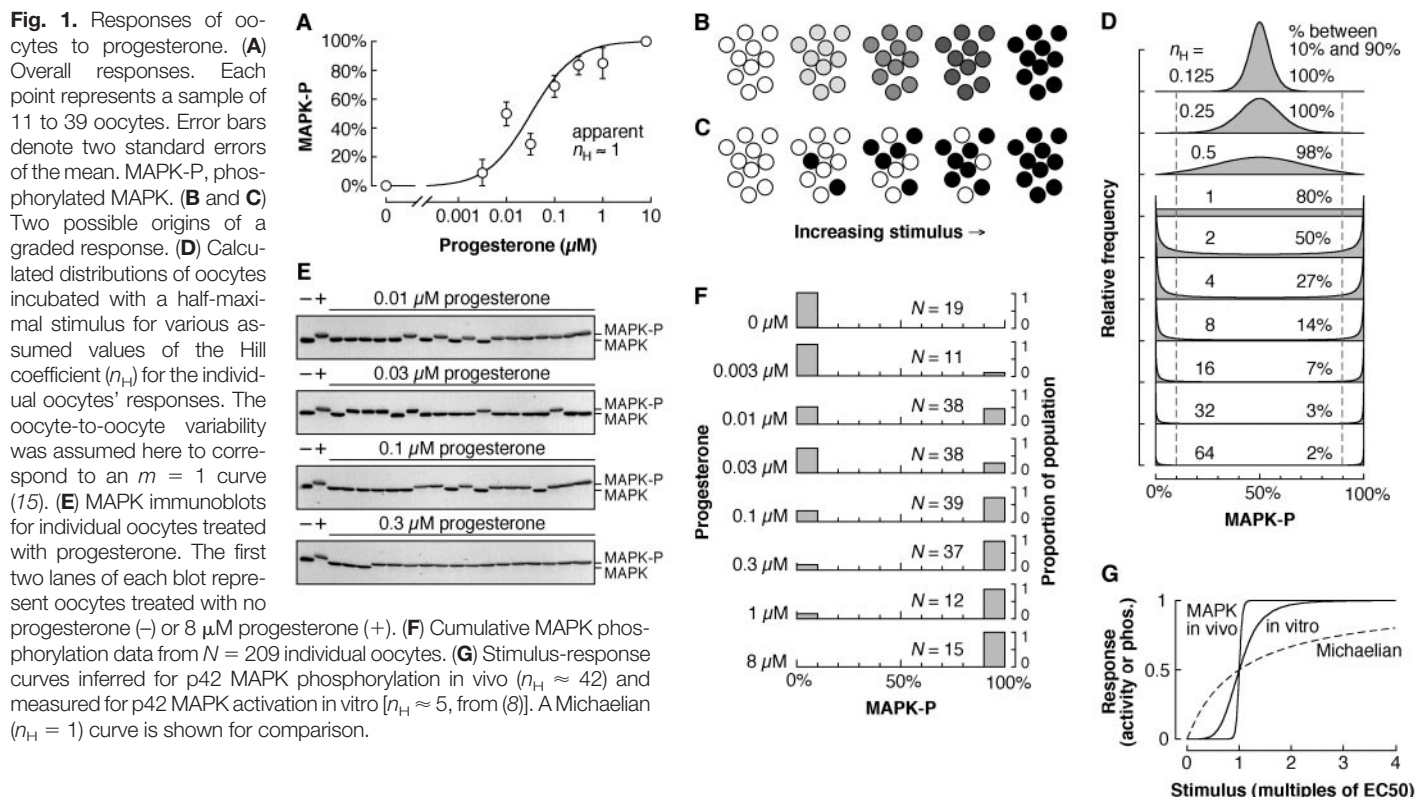
Accordingly, we examined the steady-state phosphorylation of MAPK in 190 individual progesterone-treated oocytes and 19 individual untreated oocytes. Every oocyte had either very high (>90% of maximal) or very low (<10% of maximal) amounts of MAPK phosphorylation (Fig. 1, E and F). Thus, the response of the individual oocytes was essentially all-or-none; a lower bound for the Hill coefficient was calculated to be 42 (15, 16) (Fig. 1G).

To determine whether the all-or-none character of the response was generated by

the MAPK cascade, or was passed down to the cascade by upstream signaling elements, we microinjected oocytes with purified male-Mos, a direct activator of Mek-1 (17), and assessed the resulting MAPK phosphorylation. The response of the population was steep ( $n_H > 5$ , Fig. 2A), and only one Mos-injected oocyte was found with an intermediate amount of MAPK phosphorylation (out of 89; Fig. 2, C and D). The Hill coefficient inferred for the oocytes' individual responses was about 35, similar to that for the response to progesterone. Thus, the MAPK cascade can generate, not simply propagate, a highly switchlike response to a continuously variable stimulus.

The responses seen in intact oocytes (Figs. 1 and 2) were much more switchlike than those seen in oocyte extracts (8). We hypothesized that a key difference could be a positive feedback loop known to operate in intact oocytes (4, 18–20), and known not to operate in extracts (8), whereby MAPK or something downstream from MAPK promotes the stabilization and accumulation of Mos, at least in part through the phosphorylation of Ser<sup>3</sup> (Fig. 3A) (19). A positive feedback loop would markedly increase the abruptness of the MAPK cascade's response (Fig. 3B) (21).

If protein synthesis-dependent positive feedback contributed to the highly switchlike responses seen in intact oocytes, then the protein synthesis inhibitor cyclohexi-



vide should make the response of oocytes to malE-Mos more like that seen in extracts. In agreement with this prediction, a large proportion of cycloheximide-treated, Mos-injected oocytes had intermediate amounts of MAPK phosphorylation (Fig. 2, C and D). These results imply a Hill coefficient of about 3, similar to that seen in extracts (22).

Thus, the MAPK cascade does exhibit some ultrasensitivity even when positive feedback is precluded, but protein synthesis allows a more highly switchlike response.

The intrinsic ultrasensitivity of the MAPK cascade and the protein synthesis-dependent positive feedback loop together should produce a more satisfactory switch

than either mechanism alone would. This can be seen through quantitative modeling (Fig. 3B) or simple graphical arguments (Fig. 3, C and D). If positive feedback operated and the MAPK cascade exhibited a Michaelian response to Mos, then the system would have a stable on state and an unstable off state (Fig. 3, B and C). Any nonzero level of Mos phosphorylation, added malE-Mos, or MAPK activity would trigger the feedback loop and drive the system to its on state. However, if the MAPK cascade exhibited an ultrasensitive response to Mos, then the system would have both a stable off state and a stable on state separated by a threshold (Fig. 3, B and D) (23). The ultrasensitivity of the MAPK cascade essentially filters small stimuli out of the feedback loop.

In summary, the MAPK cascade is activated in a highly ultrasensitive—essentially all-or-none—fashion during *Xenopus* oocyte maturation. This behavior is proposed to arise from two known properties of the oocyte's MAPK cascade: positive feedback, which ensures that the oocyte cannot rest in a state with intermediate MAPK phosphorylation, and the cascade's intrinsic ultrasensitivity, which establishes a threshold for activation of the positive feedback loop. Positive feedback does not appear to be uncommon, and there are many mechanisms that can give rise to ultrasensitivity (8, 9, 11, 24). Thus, other biological switches may be constructed from components that are similar or analogous to those used by the oocyte.

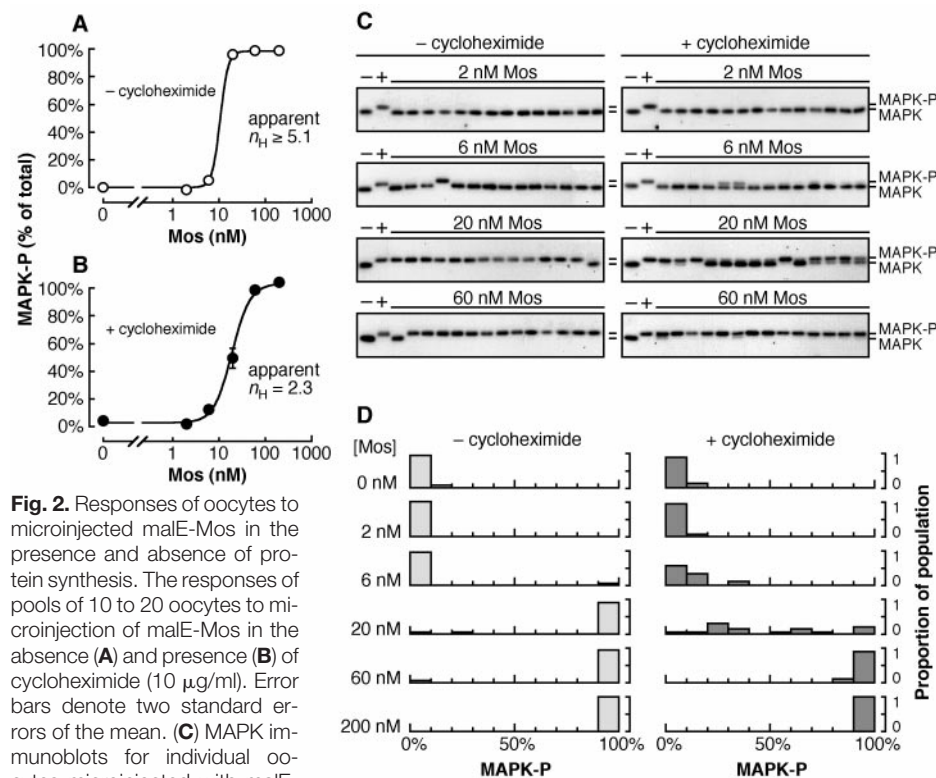


**Fig. 2.** Responses of oocytes to microinjected malE-Mos in the presence and absence of protein synthesis. The responses of pools of 10 to 20 oocytes to microinjection of malE-Mos in the absence (A) and presence (B) of cycloheximide (10  $\mu$ g/ml). Error bars denote two standard errors of the mean. (C) MAPK immunoblots for individual oocytes microinjected with malE-Mos. The first two lanes of each blot represent oocytes injected with water (-) or 200 nM malE-Mos (+). (D) Cumulative data from 202 individual oocytes.

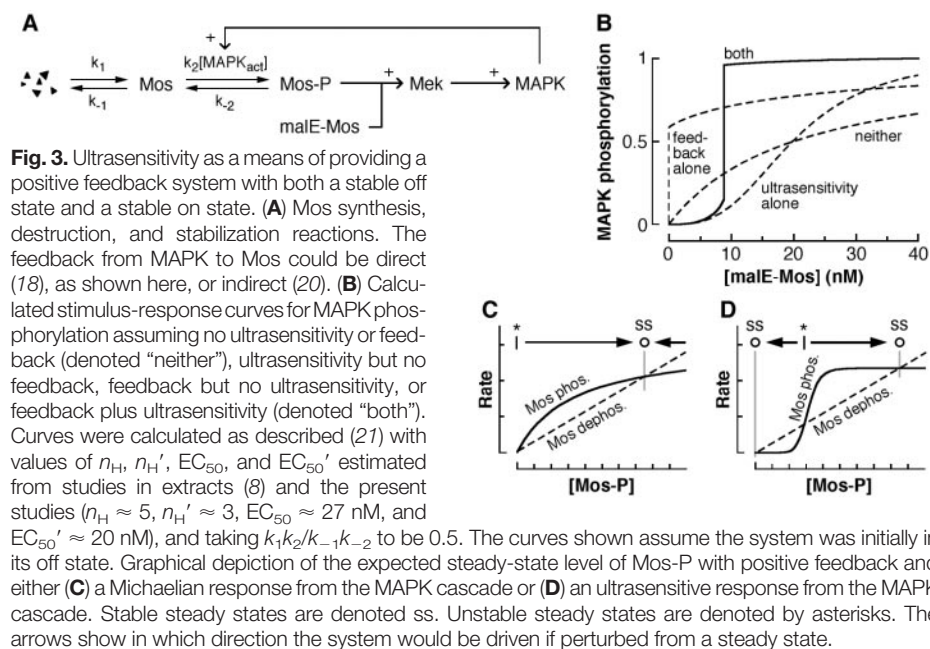


**Fig. 3.** Ultrasensitivity as a means of providing a positive feedback system with both a stable off state and a stable on state. (A) Mos synthesis, destruction, and stabilization reactions. The feedback from MAPK to Mos could be direct (18), as shown here, or indirect (20). (B) Calculated stimulus-response curves for MAPK phosphorylation assuming no ultrasensitivity or feedback (denoted "neither"), ultrasensitivity but no feedback, feedback but no ultrasensitivity, or feedback plus ultrasensitivity (denoted "both"). Curves were calculated as described (21) with values of  $\eta_H$ ,  $\eta_{H'}$ ,  $EC_{50}$ , and  $EC_{50}'$  estimated from studies in extracts (8) and the present studies ( $\eta_H \approx 5$ ,  $\eta_{H'} \approx 3$ ,  $EC_{50} \approx 27$  nM, and  $EC_{50}' \approx 20$  nM), and taking  $k_1 k_2 / k_{-1} k_{-2}$  to be 0.5. The curves shown assume the system was initially in its off state. Graphical depiction of the expected steady-state level of Mos-P with positive feedback and either (C) a Michaelian response from the MAPK cascade or (D) an ultrasensitive response from the MAPK cascade. Stable steady states are denoted ss. Unstable steady states are denoted by asterisks. The arrows show in which direction the system would be driven if perturbed from a steady state.

REFERENCES AND NOTES

1. Y. Masui, *J. Exp. Zool.* **166**, 365 (1967); W. J. Wasserman and Y. Masui, *Biol. Reprod.* **11**, 133 (1974); J. C. Gerhart, in *Biological Regulation and Development*, R. F. Goldberger, Ed. (Plenum, New York, 1980), vol. 2, pp. 133-316; N. Sagata, *Bioessays* **19**, 13 (1997); L. D. Smith, W. Xu, R. L. Varnold, *Methods Cell Biol.* **36**, 45 (1991).
2. N. Sagata, M. Oskarsson, T. Copeland, J. Brumbaugh, G. F. Vande Woude, *Nature* **335**, 519 (1988).
3. H. Kosako, Y. Gotoh, E. Nishida, *EMBO J.* **13**, 2131 (1994).
4. Y. Gotoh, N. Masuyama, K. Dell, K. Shirakabe, E. Nishida, *J. Biol. Chem.* **270**, 25898 (1995).
5. N. Yew, M. L. Mellini, G. F. Vande Woude, *Nature* **355**, 649 (1992).
6. W. Huang, D. S. Kessler, R. L. Erikson, *Mol. Biol. Cell* **6**, 237 (1995).
7. O. Haccard, A. Lewellyn, R. S. Hartley, E. Erikson, J. L. Maller, *Dev. Biol.* **168**, 677 (1995).
8. C.-Y. F. Huang and J. E. Ferrell Jr., *Proc. Natl. Acad. Sci. U.S.A.* **93**, 10078 (1996).
9. A. Goldbeter and D. E. Koshland Jr., *ibid.* **78**, 6840 (1981); D. E. Koshland Jr., A. Goldbeter, J. B. Stock, *Science* **217**, 220 (1982); A. Goldbeter and D. E. Koshland Jr., *Q. Rev. Biophys.* **15**, 555 (1982).
10. L. Stryer, *Biochemistry* (Freeman, New York, ed. 4, 1995), p. 168.
11. J. E. Ferrell Jr., *Trends Biochem. Sci.* **21**, 460 (1996).
12. W. R. Burack and T. W. Sturgill, *Biochemistry* **36**, 5929 (1997); J. E. Ferrell Jr. and R. R. Bhatt, *J. Biol. Chem.* **272**, 19008 (1997).
13. G. C. Brown, J. B. Hoek, B. N. Kholodenko, *Trends Biochem. Sci.* **22**, 288 (1997); J. E. Ferrell Jr., *ibid.*, p. 288.

14. Stage VI *Xenopus* oocytes were obtained by collagenase treatment of ovarian tissue and kept overnight in OR2 medium [82.5 mM NaCl, 2.5 mM KCl, 1 mM CaCl<sub>2</sub>, 1 mM MgCl<sub>2</sub>, 1 mM Na<sub>2</sub>HPO<sub>4</sub>, 5 mM Hepes (pH 7.8)] [R. A. Wallace, D. W. Jared, J. N. Dumont, M. W. Sega, *J. Exp. Zool.* **184**, 321 (1973)]. Oocytes were treated with progesterone or microinjected with purified recombinant malE-Mos, incubated for 8 to 10 hours, and then collected individually and frozen on dry ice. Individual oocytes were lysed by the addition of ice cold lysis buffer (50 to 100 μl) [100 mM NaCl, 50 mM β-glycerolphosphate (pH 7.4), 10 mM EDTA, 2 mM NaF, 1 mM sodium orthovanadate, leupeptin (10 μg/ml), chymostatin (10 μg/ml), and pepstatin (10 μg/ml)], and crude cytoplasm was collected after centrifugation for 2 min in a Beckman E microcentrifuge with right angle rotor. Cytoplasm was promptly added to 0.2 volumes of 6× Laemmli sample buffer. Proteins were separated on 10.5% (100:1 acrylamide:bisacrylamide) polyacrylamide SDS gels and transferred to polyvinylidene difluoride membranes. p42 MAP kinase was detected with polyclonal antiserum DC3 [K.-M. Hsiao, S.-y. Chou, S.-J. Shih, J. E. Ferrell Jr., *Proc. Natl. Acad. Sci. U.S.A.* **91**, 5480 (1994)].
15. Assume that the response  $y$  (MAPK phosphorylation or activation) of an individual oocyte to a stimulus  $x$  (progesterone or malE-Mos concentration) is well approximated by a Hill equation, as is found experimentally for MAPK responses in extracts (8):

$$y = \frac{x^{n_H}}{k^{n_H} + x^{n_H}} \quad (1)$$

Assume that individual oocytes have different values of  $k$ , which represents the concentration of  $x$  at which the oocyte's response is half-maximal, and that the distribution of oocytes among various values of  $k$  is given by

$$D = \frac{dN}{dk} \quad (2)$$

where

$$N = \frac{k^m}{a^m + k^m} \quad (3)$$

The exponent  $m$  defines the variability of the oocytes; the larger the value of  $m$ , the less variability in the concentration of stimulus at which the oocytes respond half-maximally. The constant  $a$  represents the stimulus concentration by which half of the oocytes have responded at least half-maximally. The distribution of oocytes among various values of the response  $y$  is given by

$$F = -\frac{dN}{dy} \quad (4)$$

To evaluate Eq. 4, we solve for  $k$  in terms of  $x$  and  $y$  using Eq. 1, and then substitute the result into Eq. 3:

$$k = x \left( \frac{1-y}{y} \right)^{1/n_H} \quad (5)$$

$$N = \frac{x^m \left( \frac{1-y}{y} \right)^{m/n_H}}{a^m + x^m \left( \frac{1-y}{y} \right)^{m/n_H}} \quad (6)$$

Taking the derivative of  $N$  with respect to  $y$  yields the desired formula:

$$F = \frac{-ma^m x^m \left( \frac{1-y}{y} \right)^{m/n_H}}{n \left[ a^m + x^m \left( \frac{1-y}{y} \right)^{m/n_H} \right]^2 (y-1)y} \quad (7)$$

Equation 7 describes how a population of oocytes is distributed among various values of the response  $y$  for a given level of stimulus  $x$  and given values of the steepness of the oocytes' individual responses ( $n_H$ ) and the tightness of the oocyte-to-oocyte variation ( $m$ ). This equation was used to calculate the distributions shown in Fig. 1D and to infer values of the Hill coefficient  $n_H$  for the experimentally determined oocyte distributions (Figs. 1 and 2).

16. This lower bound is calculated as the smallest Hill

coefficient for which the probability that none of the 209 oocytes will have MAPK-P between 10% and 90% is less than 0.05.

17. A. R. Nebreda and T. Hunt, *EMBO J.* **12**, 1979 (1993); J. Posada, N. Yew, N. G. Ahn, G. F. Vande Woude, J. A. Cooper, *Mol. Cell. Biol.* **13**, 2546 (1993); E. K. Shibuya and J. V. Ruderman, *Mol. Biol. Cell* **4**, 781 (1993).
18. W. T. Matten, T. D. Copeland, N. G. Ahn, G. F. Vande Woude, *Dev. Biol.* **179**, 485 (1996); L. M. Roy *et al.*, *Oncogene* **12**, 2203 (1996).
19. M. Nishizawa *et al.*, *EMBO J.* **12**, 4021 (1993).
20. Evidence that Mos accumulation depends on Cdc2 function can be found in A. R. Nebreda, J. V. Gannon, T. Hunt, *ibid.* **14**, 5597 (1995).
21. Here we shall derive an expression for the steady-state phosphorylation and activity of MAPK in response to malE-Mos for the system shown schematically in Fig. 3A. If the response of MAPK to Mos is well approximated by a Hill function with a Hill coefficient of  $n_H$  for MAPK activation and  $n_H'$  for MAPK phosphorylation, as it is in extracts (8), then the steady-state level of active MAPK is

active MAPK<sub>ss</sub> =

$$\text{MAPK}_{\text{tot}} \frac{(\text{Mos-P}_{\text{ss}} + \text{malE-Mos})^{n_H}}{\text{EC}_{50}^{n_H} + (\text{Mos-P}_{\text{ss}} + \text{malE-Mos})^{n_H}} \quad (8)$$

and the steady-state level of phosphorylated MAPK is

phos. MAPK<sub>ss</sub> =

$$\text{MAPK}_{\text{tot}} \frac{(\text{Mos-P}_{\text{ss}} + \text{malE-Mos})^{n_H'}}{\text{EC}_{50}^{n_H'} + (\text{Mos-P}_{\text{ss}} + \text{malE-Mos})^{n_H'}} \quad (9)$$

where EC<sub>50</sub> is the median effective concentration. The rate of Mos phosphorylation is  $k_2$  [MAPK<sub>active</sub>][Mos] (where the square brackets indicate concentration), and so the steady-state concentration of Mos-P is

$$\text{Mos-P}_{\text{ss}} = \frac{k_1 k_2}{k_{-1} k_{-2}} [\text{MAPK}_{\text{active}}] \quad (10)$$

Substituting Eq. 8 into Eq. 10 yields

$$\text{Mos-P}_{\text{ss}} - \left\{ \frac{k_1 k_2}{k_{-1} k_{-2}} [\text{MAPK}_{\text{tot}}] \times \frac{(\text{Mos-P}_{\text{ss}} + \text{malE-Mos})^{n_H}}{\text{EC}_{50}^{n_H} + (\text{Mos-P}_{\text{ss}} + \text{malE-Mos})^{n_H}} \right\} = 0 \quad (11)$$

The roots of this equation are the possible steady-state concentrations of Mos-P. This equation was solved numerically with Mathematica 2.2.2 (Wolfram Research, Champaign, IL). Equations 8 and 9 were then used to calculate the corresponding concentrations of active and phosphorylated MAPK (Fig. 3B). Other things being equal, as the Hill coefficient increases, the concentration of malE-Mos needed for the switching between an off state and an on state becomes larger and the "completeness" of the switching becomes greater. A Hill coefficient of 3 for MAPK phosphorylation and of 5 for MAPK activation is sufficient to produce switching with a threshold and completeness that agree well with what is observed experimentally (Fig. 3B).

22. The response of MAPK phosphorylation to malE-Mos, as measured here, is expected to exhibit a Hill coefficient of at least half that seen for the response of MAPK activation to malE-Mos, measured previously (8).
23. Bistability in other systems is discussed in B. Novak and J. J. Tyson, *J. Cell Sci.* **106**, 1153 (1993); C. D. Thron, *Biophys. Chem.* **57**, 239 (1996); J. J. Tyson, B. Novak, G. M. Odell, K. Chen, C. D. Thron, *Trends Biochem. Sci.* **21**, 89 (1996); and B. N. Kholodenko, J. B. Hoek, H. V. Westerhoff, G. C. Brown, *FEBS Lett.* **414**, 430 (1997).
24. P. B. Chock, S. G. Rhee, E. R. Stadtman, *Annu. Rev. Biochem.* **49**, 813 (1980).
25. We thank M. Murakami and G. Vande Woude for providing malE-Mos plasmids and C.-Y. F. Huang for expressing and purifying malE-Mos. Supported by a grant from NIH (GM46383) and the Stanford University Cancer Biology Training Grant (CA09302).

3 November 1997; accepted 25 March 1998

## Role of Rac1 and Oxygen Radicals in Collagenase-1 Expression Induced by Cell Shape Change

Farrah Kheradmand, Erica Werner, Patrice Tremble,\*  
Marc Symons, Zena Werb†

Integrin-mediated reorganization of cell shape leads to an altered cellular phenotype. Disruption of the actin cytoskeleton, initiated by binding of soluble antibody to α5β1 integrin, led to increased expression of the collagenase-1 gene in rabbit synovial fibroblasts. Activation of the guanosine triphosphate-binding protein Rac1, which was downstream of the integrin, was necessary for this process, and expression of activated Rac1 was sufficient to increase expression of collagenase-1. Rac1 activation generated reactive oxygen species that were essential for nuclear factor kappa B-dependent transcriptional regulation of interleukin-1α, which, in an autocrine manner, induced collagenase-1 gene expression. Remodeling of the extracellular matrix and consequent alterations of integrin-mediated adhesion and cytoarchitecture are central to development, wound healing, inflammation, and malignant disease. The resulting activation of Rac1 may lead to altered gene regulation and alterations in cellular morphogenesis, migration, and invasion.

Modifications of cell shape are crucial for tissue morphogenesis, cell migration, and invasion. These alterations in cell morphology are thought to rely on the organization of the actin cytoskeleton and the modula-

tion of cell adhesion. Changes in cell morphology lead to specific signaling from cell adhesion receptors and a consequent change of gene expression (1), including genes encoding the matrix metalloprotein-